

Cocrystallization Mechanism of Poly(3-hexyl thiophenes) with Different Amount of Chain Regioregularity

Susmita Pal, Arun K. Nandi*

Polymer Science Unit, Indian Association for the Cultivation of Science, Jadavpur, Kolkata 700032, India

Received 15 July 2005; accepted 3 January 2006

DOI 10.1002/app.24067

Published online in Wiley InterScience (www.interscience.wiley.com).

ABSTRACT: The overall crystallization rates of poly(3-hexyl thiophene) (P3HT) cocrystals with different amount of regioregularity of the components are measured using differential scanning calorimetry (DSC). Two pairs of cocrystals with varying compositions of the component polymers (viz P3HT(R) (regioregularity 92 mol %)/P3HT-2 (regioregularity 82 mol %), and P3HT-2/P3HT-1 (regioregularity 75 mol %)) are used. The crystallization rate at the same isothermal crystallization temperature (T_c) decreases with increasing regioregularity. The low Avrami exponent values (0.15–1.0) in all the samples suggest the presence of rigid amorphous portion, which cannot diffuse out quickly from the crystal growth front (soft impingement). Analysis of crystallization rate using Lauritzen–Hoffman (L–H) growth rate theory

indicates Regime I to Regime II transition in all the samples. The product of lateral and end surface energy values ($\sigma\sigma_e$) increases gradually with increasing regioregularity in the blend. Analysis of σ values indicates chain extension of the components in the melt of the blend and the entropy of activation (ΔS_{L-H}) of the cocrystals are higher than those of the components. The entropy of cocrystallization (ΔS_c) values are 1–2.4 e.u for P3HT(R)/P3HT-2 system and 0.5–1 e.u for P3HT-2/P3HT-1 system. © 2006 Wiley Periodicals, Inc. *J Appl Polym Sci* 101: 3811–3820, 2006

Key words: poly(3-hexyl thiophene); regioregularity; crystallization kinetics; chain extension factor; entropy of cocrystallization

INTRODUCTION

Poly(3-alkyl thiophenes) (P3ATs) are important members of conducting polymer family and are highly used in electronic and optoelectronic applications.¹ The polymers are not completely isoregic and have different amount of head–tail (H–T), head–head (H–H), and tail–tail (T–T) linkages^{2,3} in the chain (Scheme 1). The H–T regioregularity of the polymer chain plays an important role for both the physical and conductivity properties.^{3–5} Also the size of the alkyl group effects the above properties as well.^{6,7} In our earlier publication we have shown that the P3AT samples with same alkyl chain length can cocrystallize for a regioregularity (H–T) difference of 17 mol %.⁸ In this article we want to shed light on the cocrystallization mechanism from the crystallization rate measured by differential scanning calorimetry (DSC) technique.

There are some reports on the crystallization kinetics of the cocrystals in the literature.^{9–14} At the same

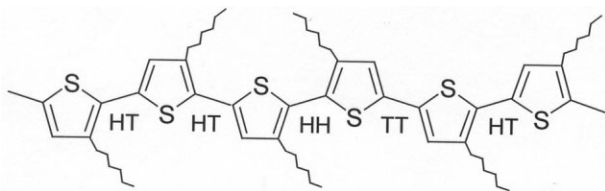
isothermal crystallization temperature (T_c) Ree observed an intermediate rate of crystallization in the cocrystals of linear low density polyethylene and ultra high molecular weight polyethylene.⁹ But Irragori et al. observed an increase in growth rate of cocrystals of linear polyethylene and branched polyethylene when compared at same T_c .¹⁰ Using time resolved Fourier transformed infrared spectroscopy (FTIR) and small angle X-ray scattering (SAXS) instruments Tashiro et al. measured the crystallization rate of polyethylene blends and observed higher crystallization rate of cocrystals at the same undercooling.^{11,12} From our laboratory, at same undercooling, similar increase in crystallization rate was observed for cocrystals of poly(vinylidene fluoride) (PVF₂) samples having different amount of head to head (H–H) defect content¹³ and also for cocrystals of vinylidene fluoride tetrafluoroethylene copolymers.¹⁴

Poly(3-hexyl thiophene) (P3HT) is an important member of P3ATs with substantial amount of head to head (H–H) defects (Scheme 1). Because of the presence of conjugated double bond and bulkier pendent group the P3HT chain is rigid. The cocrystallization mechanism of rigid chain comb-like polymers is not yet explored and in this paper attempt will be made to understand it from the crystallization kinetics study of P3HT samples. Comparison of crystallization rates, isothermal temperature range (T.R) for crystallization within same time scale, Avrami exponents (n) etc. will be made between the cocrystals and their components.

Correspondence to: A. K. Nandi (psuakn@mahendra.iacs.res.in).

Contract grant sponsor: Council of Scientific and Industrial Research, New Delhi; contract grant number: 1655/00/EMR-II

This article contains Supplementary material available at <http://www.interscience.wiley.com/jpages/0021-8995/suppmat>



Scheme 1 Poly(3-hexylthiophene) chain showing head-tail (H-T), tail-tail (T-T), and head-head (H-H) regioregularity.

It is now established from X-ray and scanning tunneling microscopy studies that P3ATs crystallize in chain folded fashion^{15,16} So the Lauritzen-Hoffman growth rate theory of chain-folded polymer crystals may be applied to analyze the kinetic data.¹⁷ The lateral surface energy (σ) and end surface energy (σ_e) of the cocrystals, evaluated from the above analysis will be used to understand the thermodynamics of the blend both at the melt and at the solid state using a recent theory of Hoffman et al.¹⁸

EXPERIMENTAL

Samples

Two types of P3HT samples e.g., regioregular and regioirregular samples were used in the work. The regioregular samples were purchased from Aldrich Chemical Co. and as reported by the company the samples were prepared by Rieke method.³ They were purified from suspended impurities by filtering their solution in chloroform. Regioirregular poly(3-hexyl thiophene) (P3HT) samples were synthesized from the chloroform solution of the monomer using anhydrous FeCl_3 as initiator under a nitrogen atmosphere.¹⁹ The polymerization temperatures were 2°C for the first set and -5°C for the second set. Polymerization was carried out for 24 h and the polymer was collected by pouring it into methanol containing 10% HCl. It was then dissolved in CHCl_3 and was filtered. The filtrate was dried by evaporation on hot plate at 60°C and finally in vacuum at 60°C for 3 days. The H-T regioregularity of the samples were measured from $^1\text{H-NMR}$ spectroscopy¹⁹ and molecular weight of the samples were measured from gel permeation chroma-

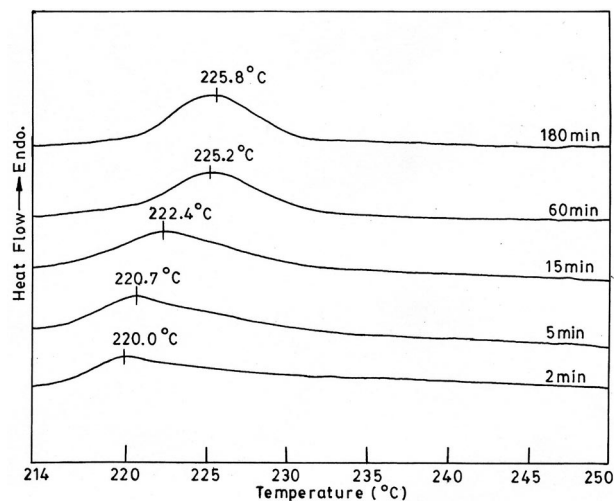


Figure 1 Representative DSC thermograms of P3HT-2/P3HT(R) blend ($W_{\text{P3HT-2}} = 0.5$) crystallized at 214°C for indicated crystallization times.

tography (Waters) using μ -stysragel column at 30°C . Polystyrene samples were chosen as standards. Blends of three different compositions of the samples were prepared by solvent-cast method using chloroform as common solvent.⁸ The characteristics of the samples used in the work are presented in Table I.

Crystallization kinetics study

The crystallization kinetics of the P3ATs and their cocrystals were measured using a differential scanning calorimeter (DSC-7, Perkin-Elmer) under nitrogen atmosphere. About 5 mg of the samples were taken in aluminum pans and were melted in DSC at 250°C and 220°C for 5 min for P3HT(R) blends and for the other blends, respectively. Then they were quenched at the rate of $200^\circ\text{C}/\text{min}$ to the predetermined isothermal crystallization temperature (T_c) where they were crystallized for different times. The samples were then heated from the T_c at the heating rate of $10^\circ/\text{min}$ without cooling. Representative melting endotherms of P3HT(R)/P3HT-2 blend for $W_{\text{P3HT-2}} = 0.5$ are shown in Figure 1 for different times of crystallization. The enthalpy of fusion (ΔH) and the

TABLE I
Characteristics of Samples Used in the Work

P3AT samples	Source	$\bar{M}_w \times 10^{-4}$	Polydispersity	Regioregularity (H-T) (mol %)	Equilibrium melting point (T_m^0) ^a ($^\circ\text{C}$)
P3HT(R)	Aldrich Chem. Co.	8.7	3.6	92	300
P3HT-1	Prepared	8.7	1.7	75	260
P3HT-2	Prepared	10.6	1.8	82	290

^a from Ref. 20.

melting points were measured by a computer attached to the instrument using PC-series DSC-7 multitasking software (version 3.2). The percentage of crystallinity was calculated from the ratio of ΔH and ΔH_u^0 taking $\Delta H_u^0 = 99 \text{ J/g}^{17}$.

RESULTS AND DISCUSSION

The cocrystallization mechanism of P3HT samples of different regioregularity is evaluated by crystallization kinetics study of blend compositions $W_x = 0.0, 0.25, 0.5, 0.75,$ and 1.0 for P3HT(R)/P3HT-2 and P3HT-2/P3HT-1 systems where W_x represents the weight fraction of the lower melting component in each blend. In Figures 2(a)–2(c) and Figures 3(a) and 2(b) the crystallization isotherms of P3HT(R)/P3HT-2 and P3HT (2)/P3HT (1) systems are shown (also supplementary Figs. 1 and 2 for other compositions). Each isotherm like the crystallization isotherms of other polymers exhibits auto catalytic nature and finally there is a retardation in the crystallization rate corresponding to the tail part of the isotherm.²¹ To understand the effect of regioregularity on isothermal crystallization temperature range (TR) in the same time scale of crystallization (1–3 decade) plots of TR versus composition of cocrystal are made and are shown in Figure 4. The TR values gradually decrease with increasing regioregular component of the blend, and there is a sudden decrease for the P3HT(R)/P3HT-2 blend at the P3HT-2-rich region. In the P3HT-2/P3HT-1 cocrystal system the decrease of TR is linear with weight fraction of lower melting component. From these results it may be surmised that the crystallization is gradually difficult with increase of regioregular P3HT sample in the blend. A clearer picture of the dependency of crystallization rate on composition can be achieved from Figure 5 where overall crystallization rate ($1/\tau_{0.01}$, $\tau_{0.01}$ is the time for 1% crystallinity in the sample), is plotted with weight fraction of lower melting component. At each isothermal temperature sharp decrease of crystallization rate with increasing weight fraction of lower melting component is observed for both the P3HT(R)/P3HT-2 and P3HT-2/P3HT-1 systems. So it may be concluded that crystallization is highly hindered with increasing regioregularity content in the blend. However, to make a thermodynamically meaningful comment on the crystallization rate of the blend, a comparison is made for crystallization at same undercooling and is shown in Figure 6. Here for the P3HT-2/P3HT-1 blend there is an increase in crystallization rate in the cocrystals than that of the components at the same undercooling ($\Delta T = 130^\circ\text{C}$). In the case of P3HT(R)/P3HT-2 blends the crystallization rate at same undercooling

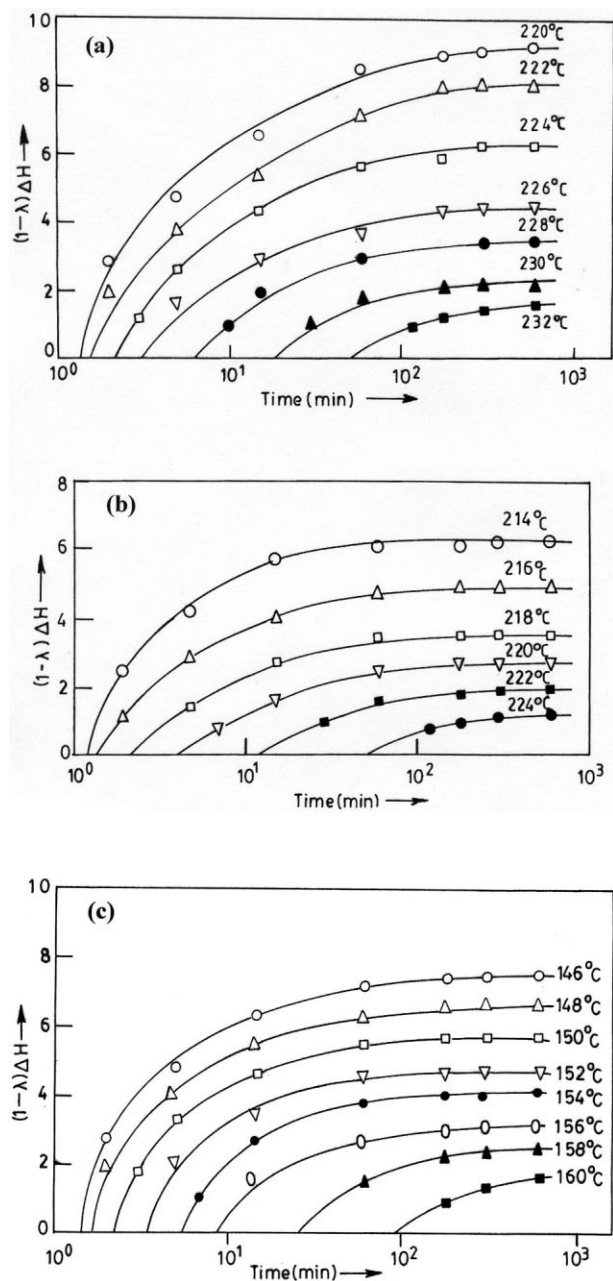


Figure 2 Crystallization isotherms at indicated temperatures of P3HT(R)/P3HT-2 systems: (a) $W_{\text{P3HT-2}} = 0.0$, (b) $W_{\text{P3HT-2}} = 0.50$, and (c) $W_{\text{P3HT-2}} = 1.0$

($\Delta T = 80^\circ\text{C}$) can not be computed for the whole blend composition, but it is clear that the crystallization rate is higher than from the line joining those of the components (shown by the dotted line). Thus it may be surmised that at the same thermodynamic condition crystallization is easier in the cocrystals than that in the pure components. From thermodynamic point of view at same undercooling the crystallization rate of the blend should be same and a possible explanation of the positive deviation from linearity of the crystallization rate will be discussed later.

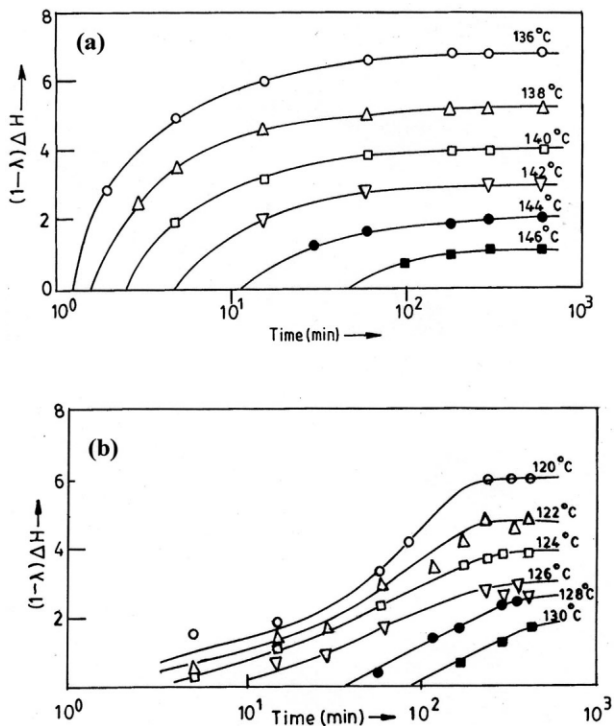


Figure 3 Crystallization isotherms at indicated temperatures of P3HT(1)/P3HT-2 systems: (a) $W_{P3HT-1} = 0.5$ and (b) $W_{P3HT-1} = 1.0$

Avrami analysis

To understand the overall crystallization mechanism the Avrami equation [eq. (1)] is applied and the n

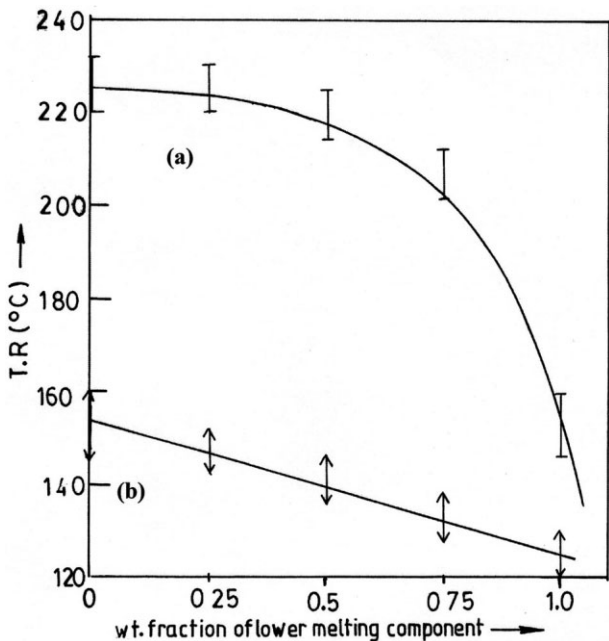


Figure 4 Isothermal temperature range (TR) for the same time scale of crystallization versus weight fraction of lower melting component: (a) P3HT(R)/P3HT-2 and (b) P3HT-1/P3HT-2 systems.

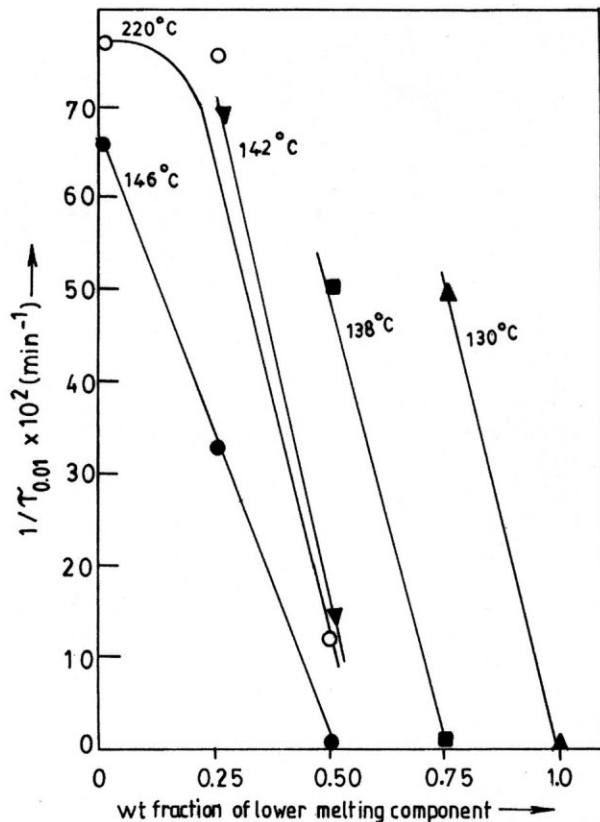


Figure 5 $1/\tau_{0.01}$ ($\tau_{0.01}$ = time to obtain 1% crystallinity, computed from Figure 2 versus weight fraction of lower melting component at indicated isothermal crystallization temperatures. Open symbol: P3HT(R)/P3HT-2 and closed symbol: P3HT-1/P3HT-2 systems.

values are calculated for the primary crystallization process. The Avrami equation²² for the nucleation and growth of a nucleus is given by:

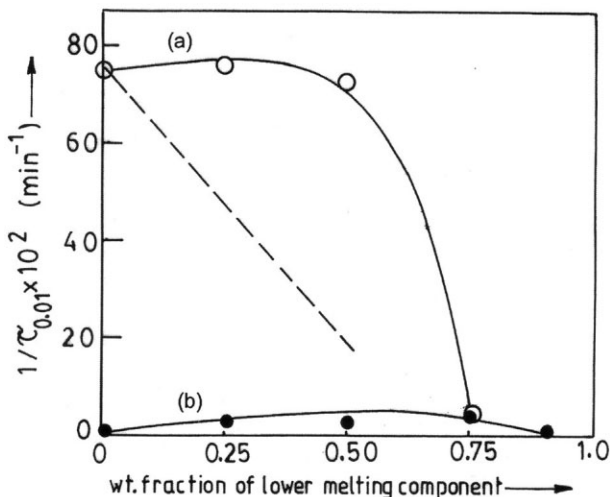


Figure 6 $1/\tau_{0.01}$ versus weight fraction of lower melting component at same undercooling: (a) P3HT(R)/P3HT-2 system ($\Delta T = 80$) and (b) P3HT-1/P3HT-2 systems ($\Delta T = 130$).

TABLE II
Values of Avrami Exponents (n) ± 0.05 for P3HT(R)/P3HT-2 and P3HT-1/P3HT-2 Systems at Different T_c Values

P3HT(R)/P3HT-2									P3HT-1/P3HT-2								
$W_X = 0.0$		$W_X = 0.25$		$W_X = 0.50$		$W_X = 0.75$		$W_X = 1.0$		$W_X = 0.25$		$W_X = 0.50$		$W_X = 0.75$		$W_X = 1.0$	
T_c (°C)	n	T_c (°C)	n	T_c (°C)	n	T_c (°C)	n	T_c (°C)	n	T_c (°C)	n	T_c (°C)	n	T_c (°C)	n	T_c (°C)	n
220	0.56	220	0.43	214	0.40	202	0.38	146	0.59	142	0.45	136	0.37	128	0.38	120	0.15
222	0.70	222	0.46	216	0.61	204	0.73	148	0.81	144	0.28	138	0.74	130	0.80	122	0.26
224	0.46	224	0.38	218	0.46	206	0.31	150	0.30	146	0.49	140	0.40	132	0.34	124	1.0
226	0.50	226	0.67	220	0.31	208	0.55	152	0.51	148	0.18	142	0.24	134	0.21	126	0.73
228	0.41	228	0.32	222	0.63	210	0.56	154	0.33	150	0.50	144	0.39	136	0.46		
230	0.43	230	0.40	224	0.27	212	0.88	156	0.58	152	0.23	146	0.55	138	0.38		

W_X = Weight fraction of lower melting component.

$$1 - \lambda(t) = 1 - \exp^{-k't^n} \quad (1)$$

where $1 - \lambda(t)$ is the crystallinity at time t , k' is the overall rate constant and n is the Avrami exponent, which denotes the nature of nucleation and growth process. The slope of double logarithmic plot of $1 - \lambda(t)$ with t at low levels of crystallinity yields the value of n .^{21,23} The n values are presented in Table II and are in the range of 0.15–1.0 for both the pure components as well as for the cocrystals. Nascimento et al. reported similar n values for crystallization of poly(3-methyl thiophene) from an electron spin resonance study.²⁴ Such low n values are usually found in condis crystals and liquid crystalline polymers.^{25–26} Recently in the crystallization of vinylidene fluoride–tetrafluoro ethylene copolymers similar low n values are also reported.²⁷

Usually for polymer crystallization n has value of 2 or 3 indicating two or three dimensional nucleation of the crystal nucleus. However, fractional values of n also exist because of secondary crystallization or crystal perfection.^{25,26} To explain the lower n values (<1) Cheng and Wunderlich²⁵ modified the Avrami equation by considering the applicability of the two assumptions of negligible nuclei volume fraction and linear crystal growth rate used in deriving eq. (1). In some rigid chain polymers and condis crystals a non-negligible volume fraction of nuclei does exist contributing an important role in the crystallization mechanism. Also in rigid chain polymers a major fraction remains as amorphous phase and can not diffuse out quickly from the crystal growth front causing a decrease in crystal growth rate (soft impingement). Considering these factors the Avrami expression has been modified as²⁵:

$$1 - \lambda(t) = 1 - \exp[-kt^{n(m+1)+p}] \quad (2)$$

where m and p are negative quantities. The negative value of m signifies that crystal growth rate (G) decreases with increase in time (t) ($G = G_0t^m$) for soft impingement and negative value of p signifies that number of active nuclei (N) decreases with increase in

time ($N(t) = N_0t^p$) because of the presence of large volume fraction of nuclei, some of them become exhausted with time. As both m and p are negative, the Avrami exponent value becomes much lesser than the conventional values of 2 or 3.

In the present system, soft impingement is occurring as there is large amount of amorphous portion ($\sim 90\%$, cf. Figs. 2 and 3) in the material arising from the rigidity of the P3AT chain. Also significant nucleation occurs through the spontaneous interdigitation of the side chains¹⁷ and these nuclei can not grow much because of rigidity of the chain yielding very low crystallinity. So from the above analysis it may be concluded that the low value of n in this system is arising from both the non-negligible volume fraction of the nuclei and also from the soft impingement of the growing crystal with the rigid amorphous portion.

Temperature coefficient analysis

To understand the microscopic mechanism of crystallization of P3HT and its cocrystals temperature coefficient analysis of the crystallization rate is necessary. P3ATs produce chain-folded crystal as evidenced from X-ray and Scanning Tunneling Microscopy.^{15,16} So Lauritzen–Hoffmann (L–H) growth rate theory of chain-folded crystals can be applied for the temperature coefficient analysis of the cocrystallization process.¹⁷ A representative model for the growth of polymer chain folded crystal is shown in Figure 7 where a surface nucleus of stem length l , thickness b and width a forms on the substrate and spreads in the direction g . The surface nucleus then completes a layer of thickness b by spreading to the crystal width L , causing the crystal to grow in the G direction. According to this theory^{28,29} the growth rate G is expressed as:

$$G = G_0 \exp[-U^*/R(T-T_\infty)] \times \exp[-K_g(i)/T(\Delta T)] \quad (3)$$

Where G_0 is the preexponential factor, U^* is the activation energy of transport, $T_\infty = T_g - 30$, T_g is the

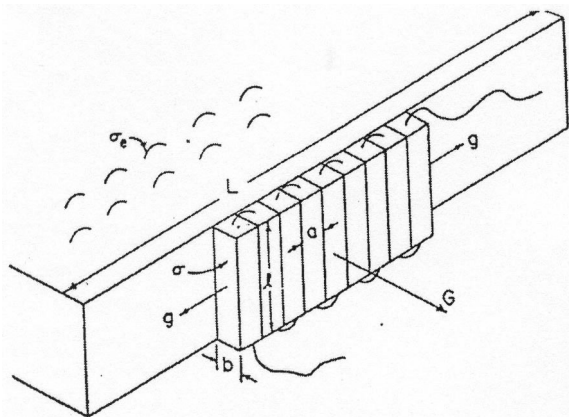


Figure 7 A representative model for the surface nucleation and growth of chain-folded crystal.

glass transition temperature, T is the crystallization temperature, $\Delta T = T_m^0 - T$ where T_m^0 is the equilibrium melting point of the crystal and $K_g(i)$ is the nucleation constant such that $K_g(\text{I}) = 2K_g(\text{II}) = K_g(\text{III})$ with $K_g(\text{I}) = 4b\sigma_e T_m^0 / k\Delta H_u^0$, σ and σ_e are lateral and end surface energies respectively, k is the Boltzmann constant and ΔH_u^0 is the enthalpy of fusion per unit volume. $K_g(\text{I})$, $K_g(\text{II})$, and $K_g(\text{III})$ represent the nucleation constants for Regime I, Regime II and Regime III crystallization. Here we consider $1/\tau_{0.01}$ to be G , where $\tau_{0.01}$ is the time required to obtain 1% crystallinity and is calculated from the crystallization isotherms at each T_c . Also the transport term contribution is neglected as the TR is very small in each sample and T_g s of the samples (4–20°C)²⁰ are also much lower than the isothermal crystallization temperatures.

In Figures 8(a) and 8(b) plots of $\ln 1/\tau_{0.01}$ versus $T_m^0/T(\Delta T)$ are shown for P3HT(R)/P3HT-2 and P3HT-2/P3HT-1 systems, respectively. It is apparent from the figure that the data points can not be presented by a single straight line and two intersecting straight lines are required to fit the data for each set. The ratio of the slopes of the two straight lines is approximately 2 in each blend. It indicates that there is Regime I to Regime II transition in each system, the Regime I crystallization takes place at higher crystallization temperatures. The regime transition temperature (T_c^*) and the undercooling of the transition for each system is presented in Table III. In both the systems it is clear that as the regioirregularity in the sample (pure or cocrystal) increases the regime transition temperature decreases. However, the undercooling at the regime transition is almost same for P3HT-2/P3HT-1 cocrystals and their components (136 ± 2). This supports that L–H theory is applicable in both the regimes for crystallization of P3HT. In the P3HT(R)/P3HT-2 system the blends also exhibit same undercooling for the regime transition except in the P3HT-2 rich region where there is some deviation.

The $\sigma\sigma_e$ values were calculated from the slopes of each straight line using eq. (3) and are presented in Table IV for both the cocrystal systems. The $\sigma\sigma_e$ values gradually increase with increasing regioirregularity in both the cocrystals as well as in the pure components. The lateral surface energy (σ) of P3HT is reported to be 12.4 erg/cm²,¹⁷ and it is assumed to be independent of chain regioirregularity. So σ_e may be calculated directly from the $\sigma\sigma_e$ values of the samples and is found to be 122.6 erg/cm² and 287.4 erg/cm² for P3HT(R) and P3HT-2, respectively. Thus with increasing irregularity in the chain the work of chain folding increases and a possible reason may be the less favorable side chain crystallization in the irregular samples producing lamellar structure.^{8,17} In the blends the σ_e values are approximated as the arithmetic average of the component values ($W_1\sigma_{e1} + W_2\sigma_{e2}$) as σ_e is the work of chain-folding and intramolecular in origin.²⁷ From

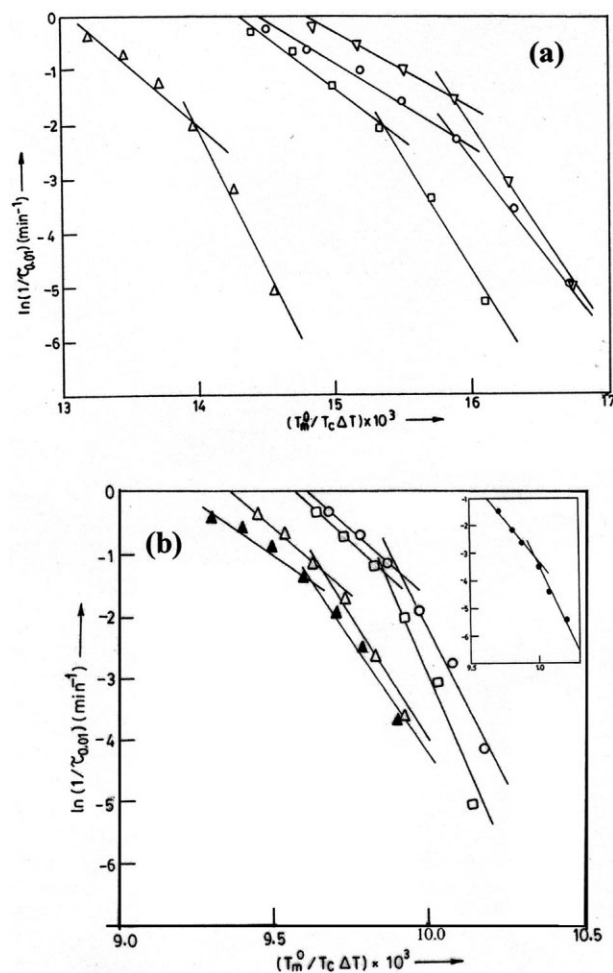


Figure 8 (a). $\ln(1/\tau_{0.01})$ versus $T_m^0/T\Delta T$ plots of P3HT(R)/P3HT-2 cocrystals at different weight fraction of the lower melting component (P3HT-2): (Δ) 0.75; (\square) 0.5; (∇) 0.25 and (\circ) 0.00. 8 (b). $\ln(1/\tau_{0.01})$ versus $T_m^0/T\Delta T$ plots of P3HT-1/P3HT-2 cocrystals at different weight fraction of the lower melting component (P3HT-1): (\blacktriangle) 0.00, (\circ) 0.75, (\square) 0.50, (Δ) 0.25. (inset- P3HT-1).

TABLE III
Equilibrium Melting Point (T_m^0)²⁰, Regime I to Regime II Transition Temperature (T_c^*) and Their Undercooling of P3HT(R)/P3HT-2 and P3HT-2/P3HT-1 Cocrystals

Sample composition (W_X) ^a	P3HT(R)/P3HT-2			P3HT-1/P3HT-2		
	T_m^0 (°C) ± 2.0	T_c^* (°C)	ΔT (°C)	T_m^0 (°C) ± 2.0	T_c^* (°C)	ΔT (°C)
0.00	300	227.9	72.1	290	152	138
0.25	298	226.0	72.0	284	146	138
0.50	295	220.0	75.0	275	140	135
0.75	292	207.9	84.1	267	132	135
1.00	290	152.0	138.0	260	126	134

^a W_X = weight fraction of lower melting component.

these σ_e values the σ values of the cocrystals are evaluated and are presented in Table IV.

The lateral surface energy (σ) may be interpreted in two different ways¹⁸:

- (i) from the chain configuration view point it relates to the chain characteristic ratio (C_α) at the melt by the relation:

$$\sigma = \Delta H_u^0(a/2)(l_b/l_u)(1/C_\alpha) \quad (4)$$

where l_b is the bond length of the monomer unit and l_u is the projected bond length of the monomeric unit along the chain direction.

- (ii) From the thermodynamic point of view, it relates to the loss of entropy for the transformation of coil (I) to the activated state (II) prior to crystallographic attachment:

$$\Delta S_{I-II} = 2b\sigma l_u n^*/T_m^0 \quad (5)$$

where n^* is the number of carbon atoms at the initial fold length (l_g^*).

Chain configuration of the melt

Here an attempt is made to understand the chain configuration of P3HT and its blends in the melt state from the lateral surface energy (σ) of their crystals. From the σ values C_α values are calculated taking $a = 16.63 \text{ \AA}$,³⁰ $\Delta H_u^0 = 10.96 \times 10^8 \text{ erg/cm}^3$ ¹⁷, $l_b/l_u = 1.26$ (calculated from energy minimized MMX model³¹). The C_α values are plotted in Figures 9(a) and 9(b) for P3HT(R)/P3HT-2 and P3HT-2/P3HT-1 systems respectively. The C_α values of the blends are higher than that of the line joining that of the component values, showing positive deviation from linearity. The C_α value of pure melt is equal to $\overline{r_0^2}/xl_b^2$ where $\overline{r_0^2}$ is the mean square unperturbed end to end distance and x is the number of the monomeric unit in the chain.³² In the melt of the cocrystals, because of the favorable interaction of the components the P3HT chains may be extended by a factor α

$$\alpha = \left(\frac{C_\alpha^{\text{Cocrystal}}}{C_\alpha^{\text{Pure}}} \right)^{1/2} \quad (6)$$

where $C_\alpha^{\text{cocrystal}}$ is the chain characteristic ratio of the cocrystal and C_α^{pure} is the C_α value for the blend composition obtained from the line joining that of the components. The α values calculated from eq. (6) are presented in Table V. From the Table it is clear that the α values are greater than unity for almost all the blends calculated from both the regimes of crystallization. Thus within the experimental accuracy it can be surmised that there is an extension of the P3HT chains in the melt of the blend, though it is small. The small extension might be arising from the dispersive interaction between the component P3HT chains at the melt of the blend. Here it should be mentioned that similar chain extension in the melt of the crystalline–amorphous^{33,34} and crystalline–crystalline blends^{13,14,35,36} are reported previously. Such chain extension in polymer blends was also predicted from Monte Carlo (MC) simulation studies by Cifra et al.^{37,38} The conclusion of the chain extension in the melt of the blend may be extended to the large amorphous portions (~90% cf. maximum crystallinity in Figs. 2 and 3) of the P3HT cocrystals where the polymer chains are somewhat extended compared to that in the pure P3HT. It is also noteworthy from Figure 9 that the C_α values of pure P3HT samples are much higher (3–4 times) than that of poly(vinylidene fluoride) samples obtained by the same method.¹³ This indicates that P3HT chains are more stiffer than poly(vinylidene fluoride) chains and it might be due to the presence both heterocyclic ring and bulkier pendent group in the chain.

Entropy of cocrystallization

During crystallization a loss of entropy of the polymer chain occurs than that in the melt state. The entropy of activation (ΔS_{I-II}) of the crystallization process has been calculated from eq. (5) taking $b = 7.75 \text{ \AA}$, $l_u = (5.03/1.26) \text{ \AA}$, and $n^* = 1.7 \times 10^{22} \text{ mL}^{-1}$ (calculated, taking $a = 16.6 \text{ \AA}$, $b = 7.75 \text{ \AA}$ and monomeric bond

TABLE IV
 $\sigma\sigma_e$ ($\text{erg}^2 \text{cm}^{-4}$); σ_e (erg cm^{-2}), and σ (erg cm^{-2}) Values of P3HT(R)/P3HT-2 and P3HT-2/P3HT-1 Cocrystals Calculated from Slopes of Figures 8(a) and 8(b) Respectively

Sample Composition (W_x)	P3HT(R)/P3HT-2				P3HT-1/P3HT-2				
	Regime I		Regime II		Regime I		Regime II		
	$\sigma\sigma_e$ ($\text{erg}^2 \text{cm}^{-4}$) ± 50	σ_e (erg cm^{-2})	σ (erg cm^{-2})	$\sigma\sigma_e$ ($\text{erg}^2 \text{cm}^{-4}$) ± 50	σ_e (erg cm^{-2})	σ (erg cm^{-2})	$\sigma\sigma_e$ ($\text{erg}^2 \text{cm}^{-4}$) ± 80	σ_e (erg cm^{-2})	σ (erg cm^{-2})
0.0	1525	122.6	12.4	1525	122.6	12.4	3757	287.4	12.4
0.25	1805	163.8	11.0 ± 0.3	1796	163.9	10.9 ± 0.4	3659	324.6	11.3 ± 0.3
0.50	2015	205.0	9.8 ± 0.3	1923	205.2	9.4 ± 0.3	5421	361.7	14.9 ± 0.3
0.75	2352	246.2	9.5 ± 0.2	2147	246.85	8.7 ± 0.2	4606	98.9	11.6 ± 0.2
1.00	3573	287.4	12.4	3578	287.8	12.4	5420	436.0	12.4
								287.8	12.4
								327.7	11.7 ± 0.3
								367.7	11.1 ± 0.3
								407.6	10.9 ± 0.3
								447.5	12.4

W_x = Weight fraction of lower melting component.

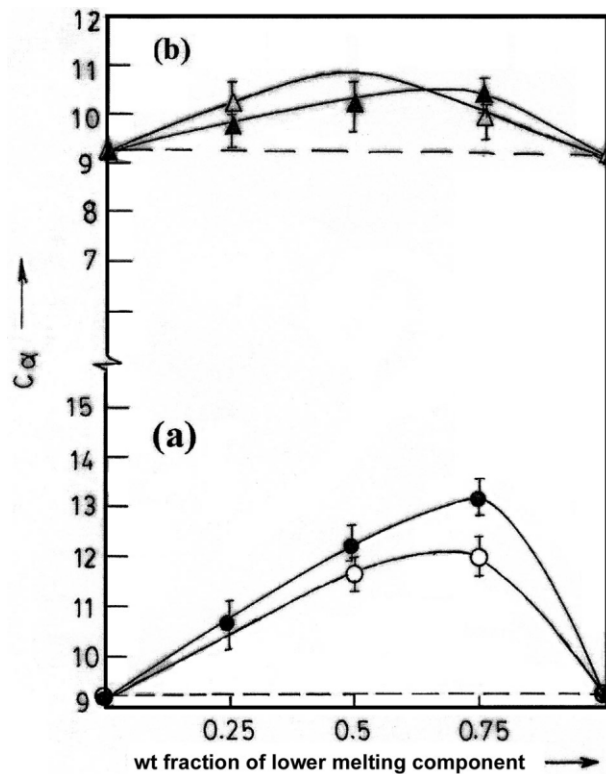


Figure 9 Plot of chain characteristic ratio (C_α) against weight fraction of lower melting component for (a) P3HT(R)/P3HT-2 and (b) P3HT-1/P3HT-2 systems. (Open symbol from Regime I data and closed symbol from Regime II data).

length, $l_b = 5.03 \text{ \AA}$). In Table V the ΔS_{I-II} values are presented and they are negative in sign signifying disorderness of the chain has decreased during the formation of activated state (localized state). In Figures 10(a) and 10(b) the entropy of activation is plotted with composition for P3HT(R)/P3HT-2 and P3HT-1/P3HT-2 systems, respectively. It is apparent from the data of both the regimes that the entropy of activation is higher for the cocrystals (according to the negative sign) than the line joining that of the components. This can be explained from the pictorial presentation of Figure 11. Pure P3HT chain has larger entropy as the chain is in coiled state with unperturbed end to end distance (r_0) but in the melt of the blend the polymer chain has lower entropy as the chains are extended by a factor α . So to produce the localized structure (activated state) entropy loss will be lesser (i.e., entropy gain is greater) in the blends than that of the pure components. In other words, there is higher entropy gain to form the activated state from the cocrystal melt and possibly it is the reason for the higher crystallization rate of the cocrystals than that of the pure components at the same undercooling.

The entropy of crystallization (ΔS_c) is calculated from Figure 10 with an approximation that the entropy change in the crystallographic attachment (State II to State III) is the same for both the pure compo-

TABLE V Chain Extension Factor (α), Entropy of Activation (ΔS_{I-II}), and Entropy of Cocrystallization ($\Delta S_{cocrystal}$) of P3HT(R)/P3HT-2 and P3HT-1/P3HT-2 Cocrystals

Cocrystal composition (W_x)*	P3HT(R)/P3HT-2			P3HT-1/P3HT-2		
	Regime I	Regime II	$\Delta S_{cocrystal}$ (e.u)	Regime I	Regime II	$\Delta S_{cocrystal}$ (e.u)
	α	ΔS_{I-II} (e.u)	$\Delta S_{cocrystal}$ (e.u)	α	ΔS_{I-II} (e.u)	$\Delta S_{cocrystal}$ (e.u)
0.00	1.00	-8.00	0.00	1.0	-8.12	0.00
0.25	1.06 ± 0.02	-7.08 ± 0.3	0.90 ± 0.3	1.05 ± 0.02	-7.50 ± 0.3	0.75 ± 0.3
0.50	1.12 ± 0.02	-6.38 ± 0.3	1.65 ± 0.3	0.91 ± 0.02	—	—
0.75	1.14 ± 0.02	-6.22 ± 0.2	1.90 ± 0.2	1.04 ± 0.02	-7.90 ± 0.2	0.55 ± 0.2
1.00	1.00	-8.12	0.00	1.00	-8.57	0.00

* weight fraction of lower melting component.

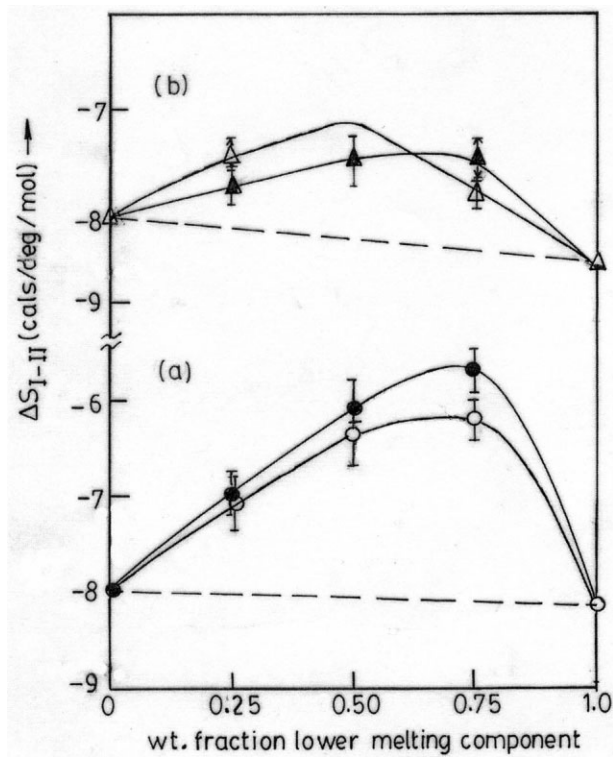


Figure 10 Plot of entropy of activation (ΔS_{I-II}) versus weight fraction of lower melting component (a) P3HT(R)/P3HT-2 and (b) P3HT-1/P3HT-2 systems. (Open symbol from Regime I data and closed symbol from Regime II data).

nents as well as for the cocrystals. Then the ΔS_c can be computed from the relation:

$$\Delta S_c = \Delta S_{I-II}^{cocrystal} - \Delta S_{I-II}^{pure} \quad (7)$$

where ΔS_{I-II}^{pure} is the entropy of activation of pure P3HT with same regioregularity as in the cocrystal but dispersity of regioregularity is smaller than that of the cocrystal (almost equal to that of the components). The ΔS_{I-II}^{pure} has been computed from the dotted line joining that of the components. ΔS_c is calculated from eq. (7) and is presented in Table V. The ΔS_c approximately ranges from 1 to 2.4 e.u and is found to increase with increasing more regioirregular component in the cocrystal for the P3HT(R)-P3HT-2 system. In the P3HT-1/P3HT-2 system the same trend of ΔS_c with composition is observed but its value (0.5–1.0 e.u) is lesser than that of the former system. The higher difference in regioregularity of the components in the former system might be the reason for higher ΔS_c value than that of the later system. So from these results it may also be concluded that cocrystallization in this system is an entropy driven process.^{13,14}

CONCLUSIONS

Both P3HT(R)/P3HT-2 and P3HT-1/P3HT-2 cocrystal systems exhibit a decrease of crystallization rate at a given T_c with increasing more regioirregular component

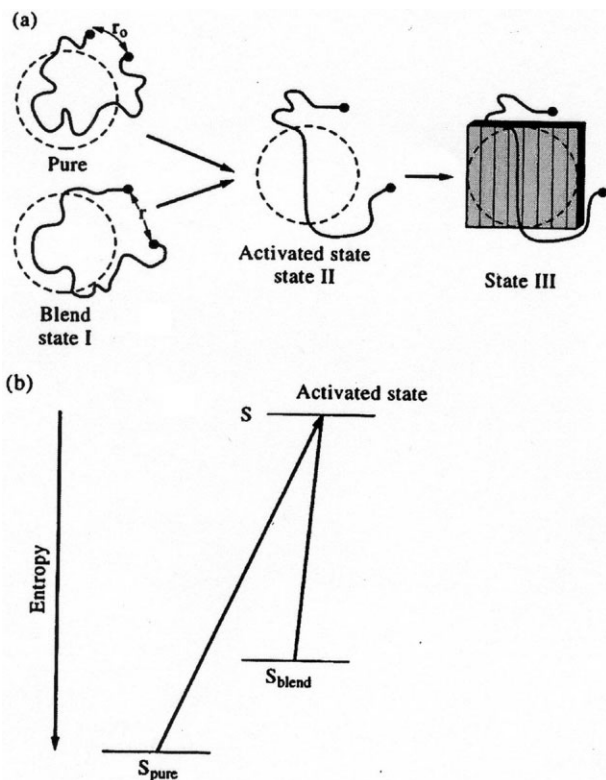


Figure 11 (a). Schematic presentation of a polymer chain for crystallographic attachment: State I coiled state, State II activated state, and State III crystallographically attached state. (b). Entropy presentation of the chain in the coiled and activated state.

in the blend. But at the same undercooling an increase of crystallization rate of the cocrystals than that of the line joining the components was observed. Avrami exponents of cocrystals are similar to those of the pure components indicating macroscopic crystallization mechanism is same for both the cocrystals and also for pure components. The low Avrami exponent values (0.2–1.0) indicate a rigid amorphous portion that cannot quickly diffuse out from the crystal growth front. Temperature coefficient analysis indicates that there is Regime I to Regime II transition in all the systems and $\sigma\sigma_e$ values gradually increase with increasing regioirregularity in the blend. An increase of σ_e value with increasing regioirregularity in the chain has been considered for the above increase. The σ values in the blends are lower than those of the component values. Analysis of σ values indicates small chain extension of the components in the melt of the blend. The entropy of activation increases in the cocrystals than that of the components. This indicates that microscopic (molecular) mechanism of crystallization of cocrystals is somewhat different than that of the pure components. The ΔS_c was found to be (1–2.4) e.u for the P3HT(R)/P3HT-2 system and (0.5–1.0) e.u for P3HT-1/P3HT-2 system indicating cocrystallization is an entropy-driven process and greater the difference in regioirregularity of the components larger is the entropy of cocrystallization.

References

- McCullough, R. D.; Ewbank, P. C. In *Handbook of Conducting Polymers*, 2nd ed.; Skotheim, T. A., Elsenbaumer, R. L., Reynolds, J. R., Eds.; Marcel Dekker: New York, 1998, p 225.
- Roncali, J. *Chem Rev* 1992, 92, 711.
- Chen, T. -A.; Wu, X.; Rieke, R. D. *J Am Chem Soc* 1995, 117, 233.
- McCullough, R. D.; Lowe, R. D.; Jayaraman, M.; Anderson, D. J. *Org Chem* 1993, 58, 904.
- Faid, K.; Frechette, M.; Ranger, M.; Mazerolle, L.; Levesque, I.; Leclerc, M.; Chen, T. A.; Reike, R. D. *Chem Mater* 1995, 7, 1930.
- Kowalik, J.; Tolbert, L. M.; Narayan, S.; Abhiraman, A. S. *Macromolecules* 2001, 34, 5471.
- Yoshino, K.; Park, D. H.; Park, B. K.; Fujii, M.; Sugimoto, R. -I. *Jpn J Appl Phys* 1988, 27, L1410.
- Pal, S.; Nandi, A. K. *Macromolecules* 2003, 36, 8426.
- Ree, M. PhD Thesis, University of Massachusetts, 1987.
- Iragorri, J. J.; Rego, J. M.; Katime, I.; Conde Brana, M. T.; Gedde, U. W. *Polymer* 1992, 33, 461.
- Tashiro, K.; Izuchi, M.; Kaneuchi, F.; Jin, C.; Kobayashi, M.; Stein, R. S. *Macromolecules* 1994, 27, 1240.
- Tashiro, K.; Imanishi, K.; Izumi, Y.; Kobayashi, M.; Kobayashi, K.; Satoh, M.; Stein, R. S. *Macromolecules* 1995, 28, 8477.
- Datta, J.; Nandi, A. K. *Polymer* 1998, 39, 1921.
- Datta, J.; Nandi, A. K. *Macromol Chem Phys* 1998, 199, 2583.
- Ihn, J. K.; Moulton, J.; Smith, P. J. *J Polym Sci Part B: Polym Phys* 1993, 31, 735.
- Mena-Osteriz, E.; Meyer, A.; Langeveld-Voss, B. M. W.; Janssen, R. A. J.; Meizer, E. W.; Bauerie, P. *Angew Chem Int Ed Engl* 2000, 39, 2680.
- Malik, S.; Nandi, A. K. *J Polym Sci Part B: Polym Phys* 2002, 40, 2073.
- Hoffman, J. D.; Miller, R. L.; Marand, H.; Rotiman, D. R. *Macromolecules* 1992, 25, 2221.
- Amou, S.; Haba, O.; Shiroto, K.; Hayakawa, T.; Ueda, M.; Takeuchi, K.; Asai, M. *J Polym Sci Part A: Polym Chem* 1999, 37, 1943.
- Pal, S.; Nandi, A. K. *J Phys Chem B* 2005, 109, 2493.
- Mandelkern, L. *Crystallization of Polymers*; McGraw-Hill: New York, 1964.
- Avrami, M. *J Chem Phys* 1939, 7, 1103.
- Avrami, M. *J Chem Phys* 1940, 8, 212.
- VonGolar, F.; Sachs, G. *Z. Phys (NY)* 1932, 77, 281.
- Nascimento, O. R.; Correa, A. A.; Bulhoes, L. O. S.; Pereira, E. C.; Puwlicke, A.; Walmsley, L. *J Chem Phys* 1998, 109, 8729.
- Cheng, S. Z. D.; Wunderlich, B. *Macromolecules* 1988, 21, 3327.
- Cheng, S. Z. D. *Macromolecules* 1988, 21, 2475.
- Datta, J.; Nandi, A. K. *Macromol Chem Phys* 1998, 199, 1583.
- Hoffman, J. D.; Weeks, J. J. *J Res Natl Bur Stand Sec A* 1962, 66, 13.
- Hoffman, J. D.; Davis, G. T.; Lauritzen, J. L., Jr. In *Treatise on Solid State Chemistry*; Hannay, N. B., Ed.; Plenum: New York, 1976; Vol. 3, p 497.
- Tashiro, K.; Ono, K.; Minagawa, Y.; Kobayashi, M.; Kawai, T.; Yoshino, K. *J Polym Sci Part B: Polym Phys* 1991, 29, 1223.
- Gajewski, K. E.; Gillbert, M. H. In *Advances in Molecular Modelling*, Liotta, D., Ed.; JAI: Greenerick, CT, 1990; Vol. 2.
- Flory, P. J. *Statistical Mechanics of Chain Molecules*; Interscience: New York, 1969.
- Huang, J.; Prasad, A.; Marand, H.; Roitman, D. B. *Polymer* 1994, 35, 1896.
- Maiti, P.; Nandi, A. K. *Polymer* 1998, 39, 413.
- Rahman, M. H.; Nandi, A. K. *Polymer* 2002, 43, 6863.
- Rahman, M. H.; Nandi, A. K. *J Polym Sci Part B: Polym Phys* 2004, 42, 2215.
- Cifra, P.; Karasz, F. E.; Macknight, W. J. *J Polym Sci Part B: Polym Phys* 1988, 26, 2379.
- Cifra, P.; Karasz, F. E.; Macknight, W. J. *Macromolecules* 1992, 25, 192.